

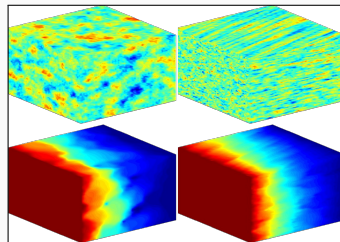
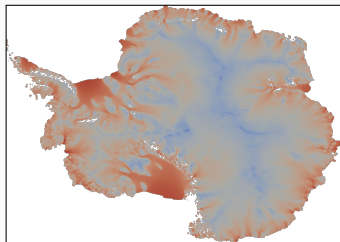
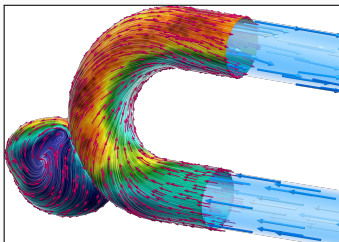
Localization via Partition of Unity Functions

Coarse Spaces for Domain Decomposition Preconditioners and Multilevel Architectures for Neural Networks

Alexander Heinlein¹

KAUST International Research Conference on Multi-Grid and Multi-Scale Methods in Computational Science, IMG 2025, KAUST, Saudi Arabia, February 3-5, 2025

¹Delft University of Technology



Numerical methods

Based on physical models

- + Robust and generalizable
- Require availability of mathematical models

Machine learning models

Driven by data

- + Do not require mathematical models
- Sensitive to data, limited extrapolation capabilities

Scientific machine learning (SciML)

Combining the strengths and compensating the weaknesses of the individual approaches:

numerical methods **improve** machine learning techniques
machine learning techniques **assist** numerical methods

1 The FROSch Package – Algebraic and Parallel Schwarz Preconditioners in TRILINOS

Based on joint work with

Axel Klawonn, Jascha Knepper, Martin Lanser, and

Lea Saßmannshausen

Mauro Perego and Siva Rajamanickam

Oliver Rheinbach and Friederik Röver

Olof Widlund

(University of Cologne)

(Sandia National Laboratories)

(TU Bergakademie Freiberg)

(New York University)

2 Multilevel domain decomposition-based architectures for physics-informed neural networks

Based on joint work with

Damien Beecroft

Victorita Dolean

Amanda A. Howard and Panos Stinis

Ben Moseley

Siddhartha Mishra

(University of Washington)

(Eindhoven University of Technology)

(Pacific Northwest National Laboratory)

(Imperial College London)

(ETH Zürich)

The FROSch Package – Algebraic and Parallel Schwarz Preconditioners in Trilinos

Solvers for Partial Differential Equations

Consider a **diffusion model problem**:

$$\begin{aligned} -\Delta u(x) &= f \quad \text{in } \Omega = [0, 1]^2, \\ u &= 0 \quad \text{on } \partial\Omega. \end{aligned}$$

Discretization using finite elements yields a **sparse** system of linear equations

$$Ku = f.$$

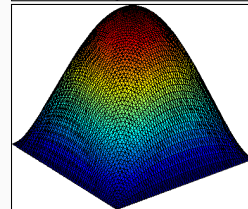
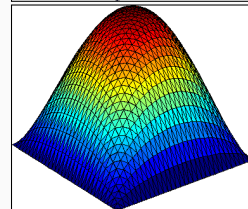
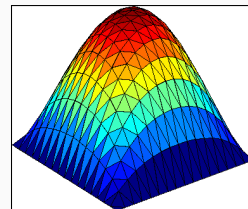
The accuracy of the finite element solution depends on the refinement level of the mesh h : **higher refinement** \Rightarrow **better accuracy**.

Direct solvers

For fine meshes, solving the system using a direct solver is not feasible due to **superlinear complexity and memory cost**.

Iterative solvers

Iterative solvers are efficient for solving **sparse systems**, however, the **convergence rate depends on the spectral properties of K** .

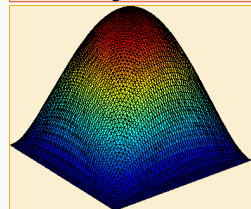
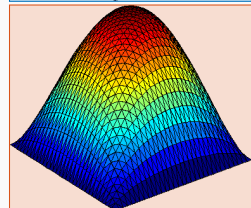
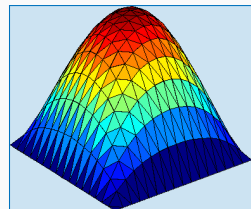
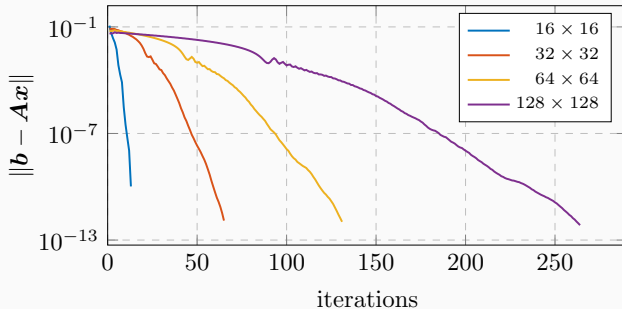


Solvers for Partial Differential Equations

Consider a **diffusion model problem**:

$$\begin{aligned} -\Delta u(x) &= f \quad \text{in } \Omega = [0, 1]^2, \\ u &= 0 \quad \text{on } \partial\Omega. \end{aligned}$$

We solve $Ku = f$ using the **conjugate gradient (CG) method**:

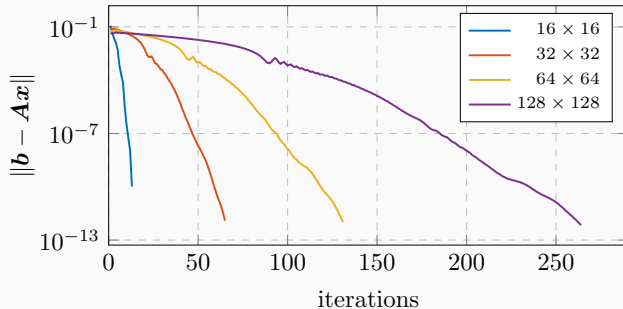


Solvers for Partial Differential Equations

Consider a **diffusion model problem**:

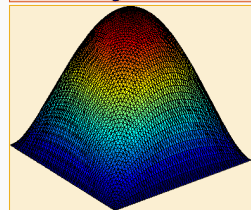
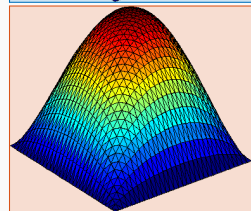
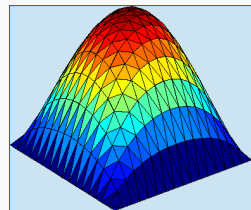
$$\begin{aligned} -\Delta u(x) &= f \quad \text{in } \Omega = [0, 1]^2, \\ u &= 0 \quad \text{on } \partial\Omega. \end{aligned}$$

We solve $Ku = f$ using the **conjugate gradient (CG) method**:



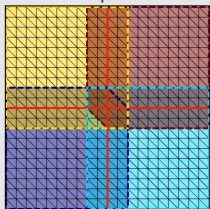
⇒ Introduce a preconditioner $M^{-1} \approx K^{-1}$ to **improve convergence**:

$$M^{-1}Ku = M^{-1}f$$

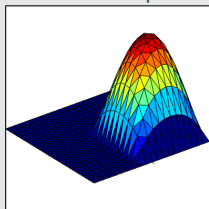


One-level Schwarz preconditioner

Overlap $\delta = 1h$



Solution of local problem



Based on an **overlapping domain decomposition**, we define a **one-level Schwarz operator**

$$M_{OS-1}^{-1}K = \sum_{i=1}^N R_i^\top K_i^{-1} R_i K,$$

where R_i and R_i^\top are restriction and prolongation operators corresponding to Ω'_i , and $K_i := R_i K R_i^\top$.

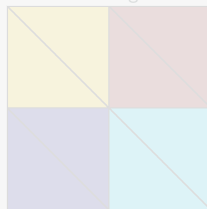
Condition number estimate:

$$\kappa(M_{OS-1}^{-1}K) \leq C \left(1 + \frac{1}{H\delta}\right)$$

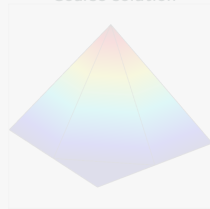
with subdomain size H and overlap width δ .

Lagrangian coarse space

Coarse triangulation



Coarse solution



The two-level overlapping Schwarz operator reads

$$M_{OS-2}^{-1}K = \underbrace{\Phi K_0^{-1} \Phi^\top K}_{\text{coarse level - global}} + \underbrace{\sum_{i=1}^N R_i^\top K_i^{-1} R_i K}_{\text{first level - local}}$$

where Φ contains the coarse basis functions and $K_0 := \Phi^\top K \Phi$; cf., e.g., **Toselli, Widlund (2005)**.

The construction of a Lagrangian coarse basis requires a coarse triangulation.

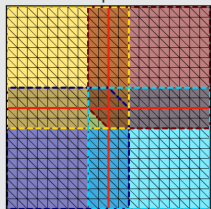
Condition number estimate:

$$\kappa(M_{OS-2}^{-1}K) \leq C \left(1 + \frac{H}{\delta}\right)$$

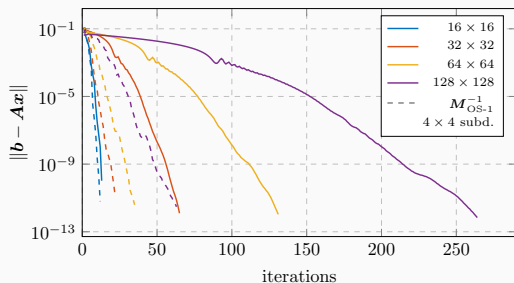
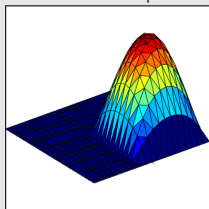
Two-Level Schwarz Preconditioners

One-level Schwarz preconditioner

Overlap $\delta = 1h$

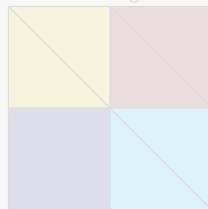


Solution of local problem

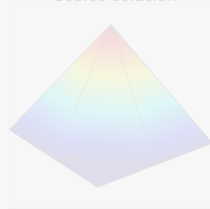


Lagrangian coarse space

Coarse triangulation



Coarse solution



The two-level overlapping Schwarz operator reads

$$M_{OS-2}^{-1}K = \underbrace{\Phi K_0^{-1} \Phi^T K}_{\text{coarse level - global}} + \underbrace{\sum_{i=1}^N R_i^T K_i^{-1} R_i K}_{\text{first level - local}}$$

where Φ contains the coarse basis functions and $K_0 := \Phi^T K \Phi$; cf., e.g., **Toselli, Widlund (2005)**.

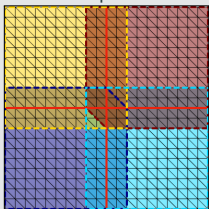
The construction of a Lagrangian coarse basis requires a coarse triangulation.

Condition number estimate:

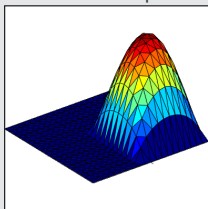
$$\kappa(M_{OS-2}^{-1}K) \leq C \left(1 + \frac{H}{\delta}\right)$$

One-level Schwarz preconditioner

Overlap $\delta = 1h$



Solution of local problem



Based on an **overlapping domain decomposition**, we define a **one-level Schwarz operator**

$$M_{OS-1}^{-1}K = \sum_{i=1}^N R_i^\top K_i^{-1} R_i K,$$

where R_i and R_i^\top are restriction and prolongation operators corresponding to Ω'_i , and $K_i := R_i K R_i^\top$.

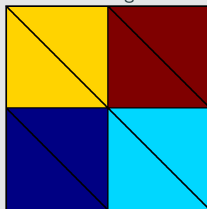
Condition number estimate:

$$\kappa(M_{OS-1}^{-1}K) \leq C \left(1 + \frac{1}{H\delta}\right)$$

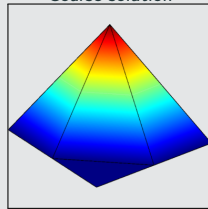
with subdomain size H and overlap width δ .

Lagrangian coarse space

Coarse triangulation



Coarse solution



The **two-level overlapping Schwarz operator** reads

$$M_{OS-2}^{-1}K = \underbrace{\Phi K_0^{-1} \Phi^\top K}_{\text{coarse level - global}} + \underbrace{\sum_{i=1}^N R_i^\top K_i^{-1} R_i K}_{\text{first level - local}}$$

where Φ contains the coarse basis functions and $K_0 := \Phi^\top K \Phi$; cf., e.g., **Toselli, Widlund (2005)**.

The construction of a Lagrangian coarse basis requires a coarse triangulation.

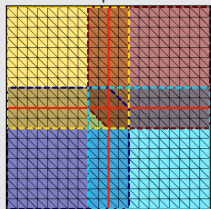
Condition number estimate:

$$\kappa(M_{OS-2}^{-1}K) \leq C \left(1 + \frac{H}{\delta}\right)$$

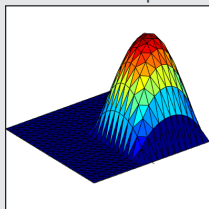
Two-Level Schwarz Preconditioners

One-level Schwarz preconditioner

Overlap $\delta = 1h$

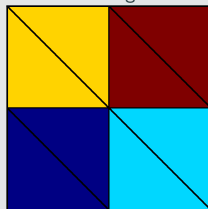


Solution of local problem

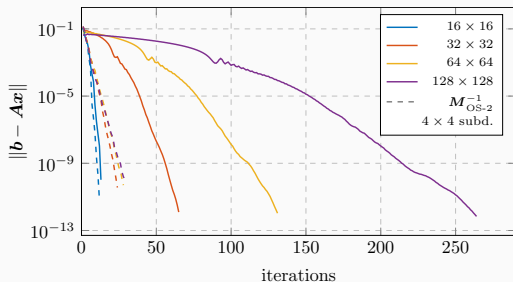
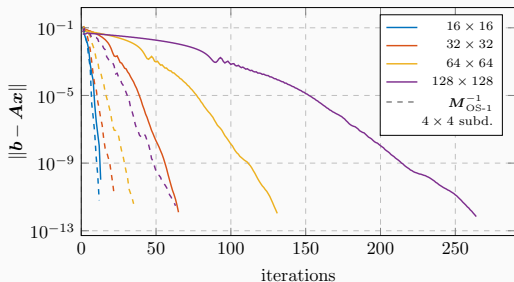
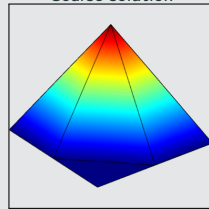


Lagrangian coarse space

Coarse triangulation



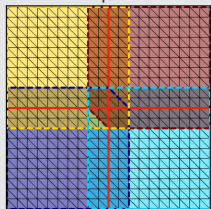
Coarse solution



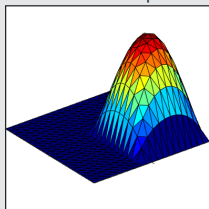
Two-Level Schwarz Preconditioners

One-level Schwarz preconditioner

Overlap $\delta = 1h$

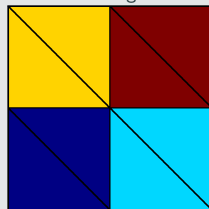


Solution of local problem

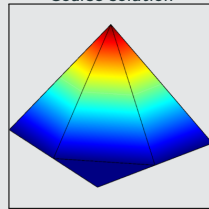


Lagrangian coarse space

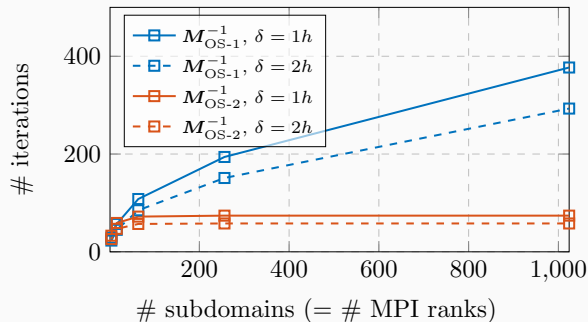
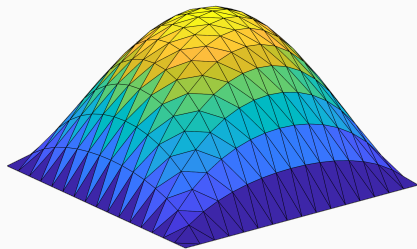
Coarse triangulation



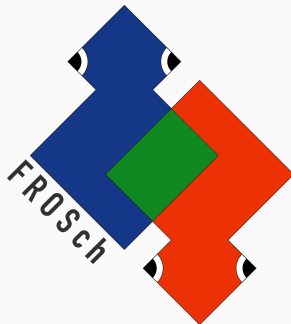
Coarse solution



Diffusion model problem in two dimensions,
 $H/h = 100$



FROSch (Fast and Robust Overlapping Schwarz) Framework in Trilinos



Sandia
National
Laboratories



TUBAF
Die Ressourcenuniversität.
Seit 1765.

Software

- Object-oriented C++ domain decomposition solver framework with MPI-based distributed memory parallelization
- Part of TRILINOS with support for both parallel linear algebra packages EPETRA and TPETRA
- Node-level parallelization and performance portability on CPU and GPU architectures through KOKKOS and KOKKOSKERNELS
- Accessible through unified TRILINOS solver interface STRATIMIKOS

Methodology

- **Parallel scalable multi-level Schwarz domain decomposition preconditioners**
- **Algebraic construction** based on the parallel distributed system matrix
- **Extension-based coarse spaces**

Team (active)

- Filipe Cumaru (TU Delft)
- Kyrill Ho (UCologne)
- Jascha Knepper (UCologne)
- Friederike Röver (TUBAF)
- Lea Saßmannshausen (UCologne)
- Alexander Heinlein (TU Delft)
- Axel Klawonn (UCologne)
- Siva Rajamanickam (SNL)
- Oliver Rheinbach (TUBAF)
- Ichitaro Yamazaki (SNL)

Partition of Unity

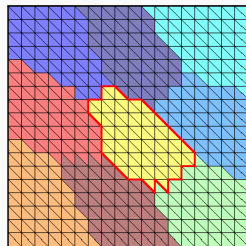
The **energy-minimizing extension** $v_i = H_{\partial\Omega_i \rightarrow \Omega_i}(v_{i, \partial\Omega_i})$ solves

$$\begin{aligned} -\Delta v_i &= 0 && \text{in } \Omega_i, \\ v_i &= v_{i, \partial\Omega_i} && \text{on } \partial\Omega_i. \end{aligned}$$

Hence, $v_i = E_{\partial\Omega_i \rightarrow \Omega_i}(\mathbb{1}_{\partial\Omega_i}) = \mathbb{1}$.

Due to **linearity of the extension operator**, we have

$$\sum_i \varphi_i = \mathbb{1}_{\partial\Omega_i} \Rightarrow \sum_i E_{\partial\Omega_i \rightarrow \Omega_i}(\varphi_i) = \mathbb{1}_{\Omega_i}$$



Null space property

Any extension-based coarse space built from a partition of unity on the domain decomposition interface satisfies the **null space property necessary for numerical scalability**:

$$\sum_{\text{edges } \subset \partial\Omega_i} \text{[3D plot of a peak on an edge]} + \sum_{\text{vertices } \subset \partial\Omega_i} \text{[3D plot of a peak on a vertex]} = \text{[3D plot of a peak on the entire interface]}$$

Algebraicity of the energy-minimizing extension

The computation of energy-minimizing extensions only requires K_{II} and $K_{I\Gamma}$, **submatrices of the fully assembled matrix K_i** .

$$\mathbf{v} = \begin{bmatrix} -K_{II}^{-1} K_{I\Gamma} \\ I_{\Gamma} \end{bmatrix} \mathbf{v}_{\Gamma},$$

Overlapping domain decomposition

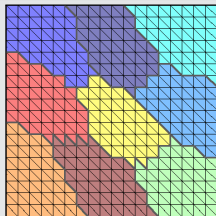
The **overlapping subdomains** are constructed by **recursively adding layers of elements** via the sparsity pattern of K .

The corresponding matrices

$$K_i = R_i K R_i^T$$

can easily be extracted from K .

Nonoverlapping DD



Overlapping domain decomposition

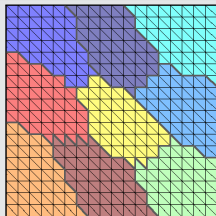
The **overlapping subdomains** are constructed by **recursively adding layers of elements** via the sparsity pattern of K .

The corresponding matrices

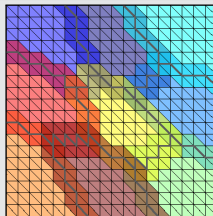
$$K_i = R_i K R_i^T$$

can easily be extracted from K .

Nonoverlapping DD



Overlap $\delta = 1h$



Overlapping domain decomposition

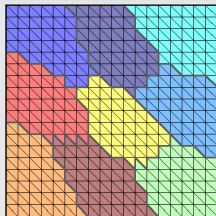
The **overlapping subdomains** are constructed by **recursively adding layers of elements** via the sparsity pattern of \mathbf{K} .

The corresponding matrices

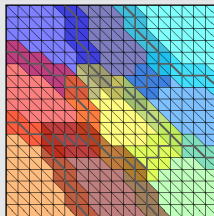
$$\mathbf{K}_i = \mathbf{R}_i \mathbf{K} \mathbf{R}_i^T$$

can easily be extracted from \mathbf{K} .

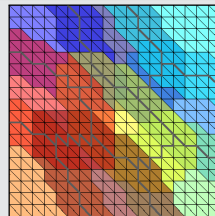
Nonoverlapping DD



Overlap $\delta = 1h$



Overlap $\delta = 2h$



Overlapping domain decomposition

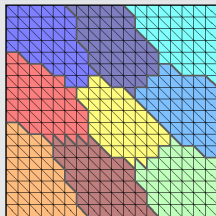
The **overlapping subdomains** are constructed by **recursively adding layers of elements** via the sparsity pattern of K .

The corresponding matrices

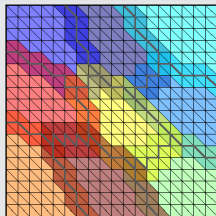
$$K_i = R_i K R_i^T$$

can easily be extracted from K .

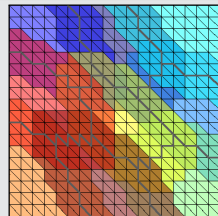
Nonoverlapping DD



Overlap $\delta = 1h$

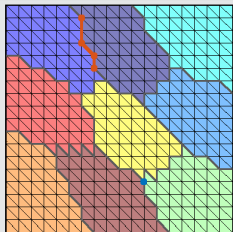


Overlap $\delta = 2h$



Coarse space

1. Interface components



Overlapping domain decomposition

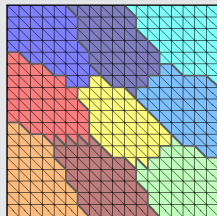
The **overlapping subdomains** are constructed by **recursively adding layers of elements** via the sparsity pattern of K .

The corresponding matrices

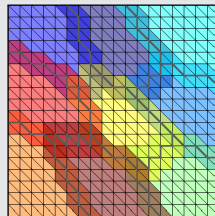
$$K_i = R_i K R_i^T$$

can easily be extracted from K .

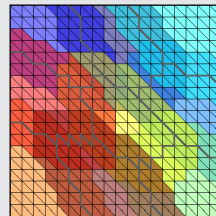
Nonoverlapping DD



Overlap $\delta = 1h$

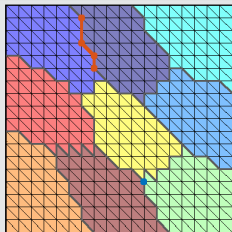


Overlap $\delta = 2h$

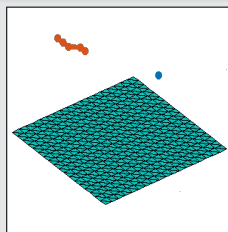


Coarse space

1. Interface components



2. Interface basis (partition of unity \times null space)



For **scalar elliptic problems**, the **null space** consists only of **constant functions**.

Overlapping domain decomposition

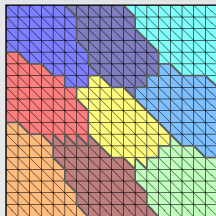
The **overlapping subdomains** are constructed by **recursively adding layers of elements** via the sparsity pattern of K .

The corresponding matrices

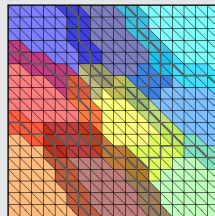
$$K_i = R_i K R_i^T$$

can easily be extracted from K .

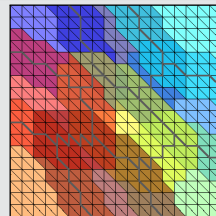
Nonoverlapping DD



Overlap $\delta = 1h$

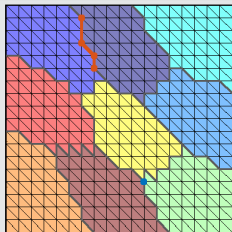


Overlap $\delta = 2h$

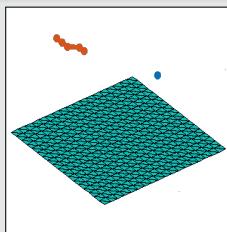


Coarse space

1. Interface components

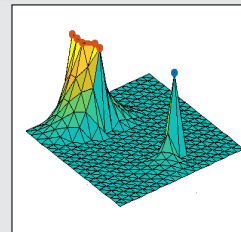


2. Interface basis (partition of unity \times null space)



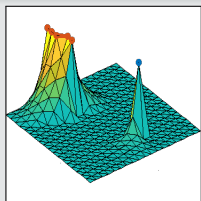
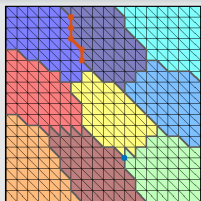
For scalar elliptic problems, the null space consists only of constant functions.

3. Extension



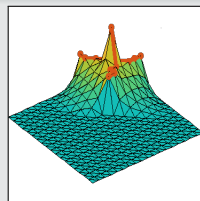
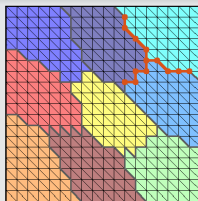
Examples of FROSch Coarse Spaces

GDSW (Generalized Dryja–Smith–Widlund)



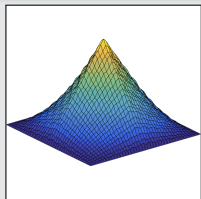
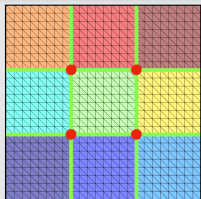
- Dohrmann, Klawonn, Widlund (2008)
- Dohrmann, Widlund (2009, 2010, 2012)

RGDSW (Reduced dimension GDSW)



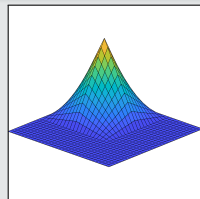
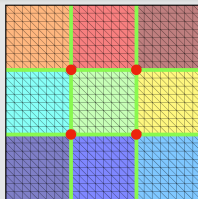
- Dohrmann, Widlund (2017)
- H., Klawonn, Knepper, Rheinbach, Widlund (2022)

MsFEM (Multiscale Finite Element Method)



- Hou (1997), Efendiev and Hou (2009)
- Buck, Iliev, and Andrä (2013)
- H., Klawonn, Knepper, Rheinbach (2018)

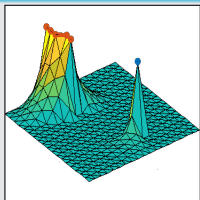
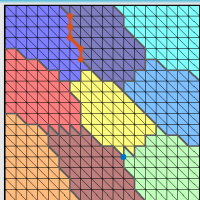
Q1 Lagrangian / piecewise bilinear



Piecewise linear interface partition of unity functions and a structured domain decomposition.

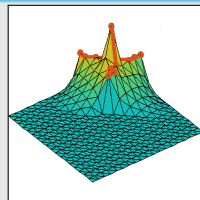
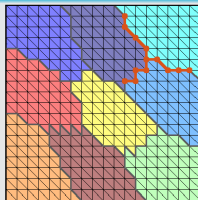
Examples of FROSch Coarse Spaces

GDSW (Generalized Dryja–Smith–Widlund)



- Dohrmann, Klawonn, Widlund (2008)
- Dohrmann, Widlund (2009, 2010, 2012)

RGDSW (Reduced dimension GDSW)



- Dohrmann, Widlund (2017)
- H., Klawonn, Knepper, Rheinbach, Widlund (2022)

For elliptic model problems, the **condition number of the (R)GDSW two-level Schwarz operator** is bounded by

$$\kappa \left(M_{(\text{R})\text{GDSW}}^{-1} \mathbf{K} \right) \leq C \left(1 + \frac{H}{\delta} \right) \left(1 + \log \left(\frac{H}{h} \right) \right)^\alpha,$$

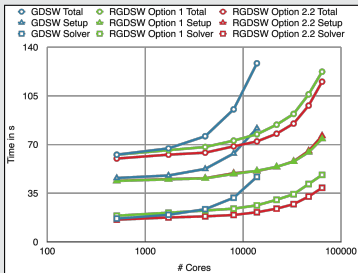
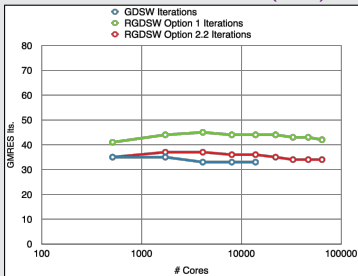
where

- C constant (does not depend on h , H , or δ),
- H subdomain diameter,
- h element size,
- δ width of the overlap,
- $\alpha \in \{0, 1, 2\}$ power (depends on problem dimension, regularity of the subdomains, and variant of the algorithm).

Weak Scalability up to 64k MPI Ranks / 1.7b Unknowns (3D Poisson; Juqueen)

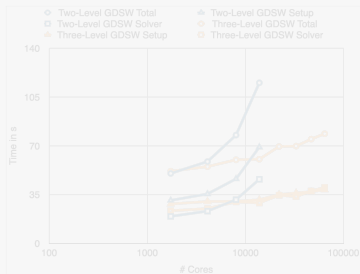
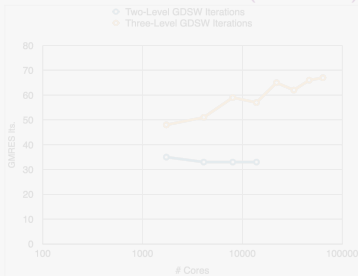
GDSW vs RGDSW (reduced dimension)

Heinlein, Klawonn, Rheinbach, Widlund (2019).



Two-level vs three-level GDSW

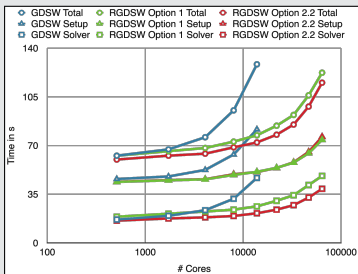
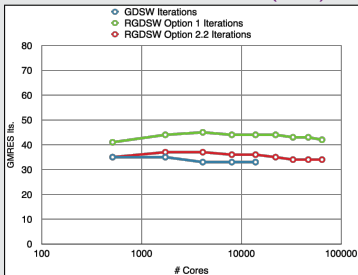
Heinlein, Klawonn, Rheinbach, Röver (2019, 2020).



Weak Scalability up to 64k MPI Ranks / 1.7b Unknowns (3D Poisson; Juqueen)

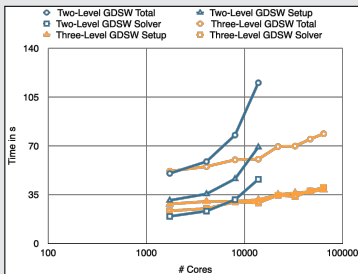
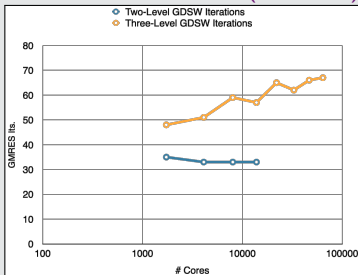
GDSW vs RGDSW (reduced dimension)

Heinlein, Klawonn, Rheinbach, Widlund (2019).



Two-level vs three-level GDSW

Heinlein, Klawonn, Rheinbach, Röer (2019, 2020).



Monolithic (R)GDSW Preconditioners for CFD Simulations

Consider the discrete saddle point problem

$$\mathcal{A}x = \begin{bmatrix} \mathbf{K} & \mathbf{B}^\top \\ \mathbf{B} & \mathbf{0} \end{bmatrix} \begin{bmatrix} \mathbf{u} \\ \mathbf{p} \end{bmatrix} = \begin{bmatrix} \mathbf{f} \\ \mathbf{0} \end{bmatrix} = \mathbf{b}.$$

Monolithic GDSW preconditioner

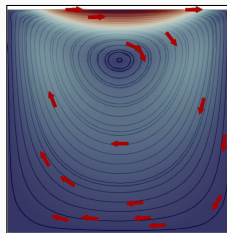
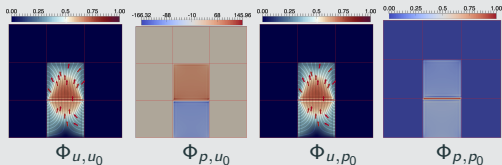
We construct a **monolithic GDSW preconditioner**

$$m_{\text{GDSW}}^{-1} = \phi \mathcal{A}_0^{-1} \phi^\top + \sum_{i=1}^N \mathcal{R}_i^\top \bar{\mathcal{P}}_i \mathcal{A}_i^{-1} \mathcal{R}_i,$$

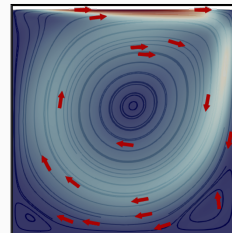
with block matrices $\mathcal{A}_0 = \phi^\top \mathcal{A} \phi$, $\mathcal{A}_i = \mathcal{R}_i \mathcal{A} \mathcal{R}_i^\top$,
local pressure projections $\bar{\mathcal{P}}_i$, and

$$\mathcal{R}_i = \begin{bmatrix} \mathcal{R}_{u,i} & \mathbf{0} \\ \mathbf{0} & \mathcal{R}_{p,i} \end{bmatrix} \quad \text{and} \quad \phi = \begin{bmatrix} \Phi_{u,u_0} & \Phi_{u,p_0} \\ \Phi_{p,u_0} & \Phi_{p,p_0} \end{bmatrix}.$$

Using \mathcal{A} to compute extensions: $\phi_l = -\mathcal{A}_{ll}^{-1} \mathcal{A}_{l\Gamma} \phi_\Gamma$;
cf. **Heinlein, Hochmuth, Klawonn (2019, 2020)**.



Stokes flow

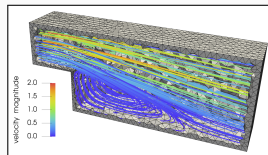
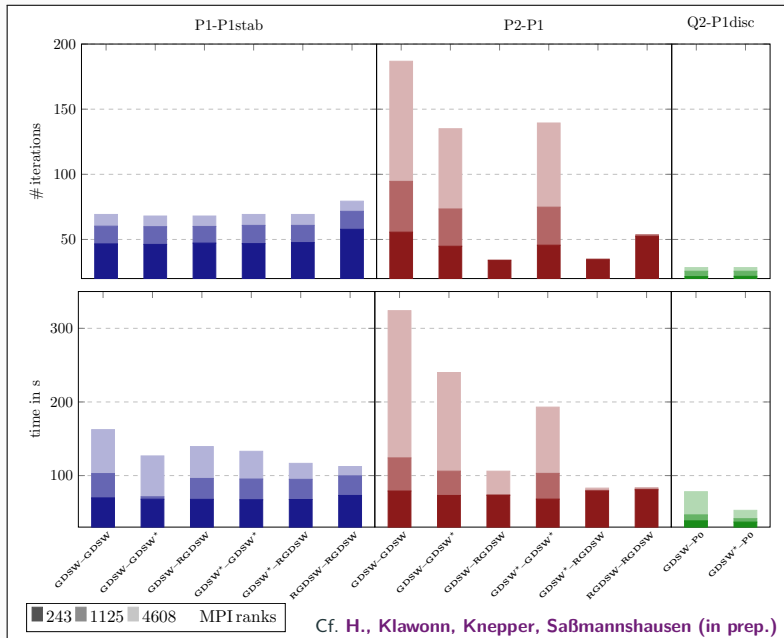


Navier–Stokes flow

Related work:

- Original work on monolithic Schwarz preconditioners: **Klawonn and Pavarino (1998, 2000)**
- Other publications on monolithic Schwarz preconditioners: e.g., **Hwang and Cai (2006)**, **Barker and Cai (2010)**, **Wu and Cai (2014)**, and the presentation **Dohrmann (2010)** at the *Workshop on Adaptive Finite Elements and Domain Decomposition Methods in Milan*.

Balancing the Velocity and Pressure Coarse Spaces

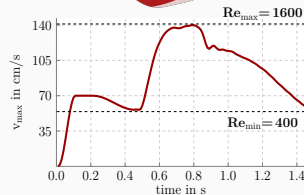
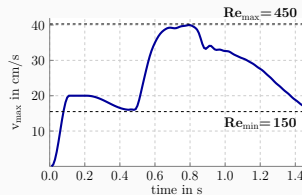
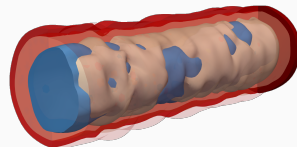


Varying the POU



Results for Blood Flow Simulations

- **3D unsteady flow simulation** within the **geometry of a realistic artery** (from **Balzani et al. (2012)**) and kinematic viscosity $\nu = 0.03 \text{ cm}^2/\text{s}$
- **Parabolic inflow profile** is prescribed at inlet of geometry
- **Time discretization:** BDF-2; **space discretization:** P2-P1 elements



prec.	# MPI ranks	16	64	256
Monolithic RGDSW (FRO _{SCH})	avg. #its.	33	31	30
	setup	4 825 s	1 422 s	701 s
	solve	3 198 s	1 004 s	463 s
	total	8 023 s	2 426 s	1 164 s
SIMPLE RGDSW (TEKO & FRO _{SCH})	avg. #its.	82	82	87
	setup	3 046 s	824 s	428 s
	solve	4 679 s	1 533 s	801 s
	total	7 725 s	2 357 s	1 229 s

prec.	# MPI ranks	16	64	256
Monolithic RGDSW (FRO _{SCH})	avg. #its.	36	36	36
	setup	4 808 s	1 448 s	688 s
	solve	3 490 s	1 186 s	538 s
	total	8 298 s	2 634 s	1 226 s
SIMPLE RGDSW (TEKO & FRO _{SCH})	avg. #its.	157	164	169
	setup	3 071 s	842 s	432 s
	solve	9 541 s	3 210 s	1 585 s
	total	12 612 s	4 052 s	2 017 s

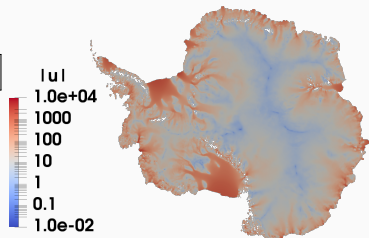


<https://github.com/SNLComputation/Albany>

The velocity of the ice sheet in Antarctica and Greenland is modeled by a **first-order-accurate Stokes approximation model**,

$$-\nabla \cdot (2\mu\dot{\epsilon}_1) + \rho g \frac{\partial s}{\partial x} = 0, \quad -\nabla \cdot (2\mu\dot{\epsilon}_2) + \rho g \frac{\partial s}{\partial y} = 0,$$

with a **nonlinear viscosity model** (Glen's law); cf., e.g., **Blatter (1995)** and **Pattyn (2003)**.



MPI ranks	Antarctica (velocity)			Greenland (multiphysics vel. & temperature)		
	4 km resolution, 20 layers, 35 m dofs			1-10 km resolution, 20 layers, 69 m dofs		
	avg. its	avg. setup	avg. solve	avg. its	avg. setup	avg. solve
512	41.9 (11)	25.10 s	12.29 s	41.3 (36)	18.78 s	4.99 s
1 024	43.3 (11)	9.18 s	5.85 s	53.0 (29)	8.68 s	4.22 s
2 048	41.4 (11)	4.15 s	2.63 s	62.2 (86)	4.47 s	4.23 s
4 096	41.2 (11)	1.66 s	1.49 s	68.9 (40)	2.52 s	2.86 s
8 192	40.2 (11)	1.26 s	1.06 s	-	-	-

Computations performed on Cori (NERSC).

Heinlein, Perego, Rajamanickam (2022)

Linear & Nonlinear Preconditioning

Let us consider the nonlinear problem arising from the discretization of a partial differential equation

$$\mathbf{F}(\mathbf{u}) = 0.$$

We solve the problem using a **Newton-Krylov approach**, i.e., we solve a sequence of linearized problems using a Krylov subspace method:

$$-DF(\mathbf{u}^{(k)}) \Delta \mathbf{u}^{(k+1)} = \mathbf{F}(\mathbf{u}^{(k)}).$$

Linear preconditioning

In linear preconditioning, we **improve the convergence speed of the linear solver** by constructing a **linear operator** M^{-1} and solve linear systems

$$-M^{-1}DF(\mathbf{u}^{(k)}) \Delta \mathbf{u}^{(k+1)} = M^{-1}\mathbf{F}(\mathbf{u}^{(k)}).$$

Goal:

- $\kappa(M^{-1}DF(\mathbf{u}^{(k)})) \approx 1.$
- $$\Rightarrow M^{-1}DF(\mathbf{u}^{(k)}) \approx I.$$

Nonlinear preconditioning

In nonlinear preconditioning, we **improve the convergence speed of the nonlinear solver** by constructing a **nonlinear operator** G and solve the nonlinear system

$$(G \circ F)(\mathbf{u}) = 0.$$

Goals:

- $G \circ F$ almost linear.
- Additionally: $\kappa(D(G \circ F)(\mathbf{u})) \approx 1.$

Linear & Nonlinear Preconditioning

Let us consider the nonlinear problem arising from the discretization of a partial differential equation

$$\mathbf{F}(\mathbf{u}) = 0.$$

We solve the problem using a **Newton-Krylov approach**, i.e., we solve a sequence of linearized problems using a Krylov subspace method:

$$-DF(\mathbf{u}^{(k)}) \Delta \mathbf{u}^{(k+1)} = \mathbf{F}(\mathbf{u}^{(k)}).$$

Linear preconditioning

In linear preconditioning, we **improve the convergence speed of the linear solver** by constructing a **linear operator** M^{-1} and solve linear systems

$$-M^{-1}DF(\mathbf{u}^{(k)}) \Delta \mathbf{u}^{(k+1)} = M^{-1}\mathbf{F}(\mathbf{u}^{(k)}).$$

Goal:

- $\kappa(M^{-1}DF(\mathbf{u}^{(k)})) \approx 1.$
- $$\Rightarrow M^{-1}DF(\mathbf{u}^{(k)}) \approx I.$$

Nonlinear preconditioning

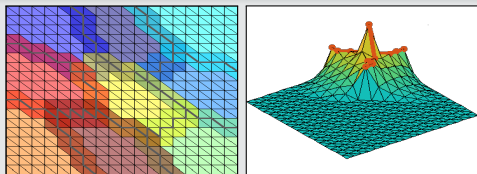
In nonlinear preconditioning, we **improve the convergence speed of the nonlinear solver** by constructing a **nonlinear operator** G and solve the nonlinear system

$$(G \circ F)(\mathbf{u}) = 0.$$

Goals:

- $G \circ F$ almost linear.
- Additionally: $\kappa(D(G \circ F)(\mathbf{u})) \approx 1.$

ASPEN & ASPIN methods



In additive Schwarz preconditioned (in)exact Newton (ASPEN/ASPIN) (Cai and Keyes (2002)), the nonlinear problem

$$F(u) = 0$$

is reformulated as the equivalent problem

$$\sum_{i=1}^N P_i T_i(u) = 0$$

with corrections $T_i(u)$ given by nonlinear problems on the overlapping subdomains

$$R_i F(u - P_i T_i(u)) = 0.$$

R_i restriction; P_i prolongation.

Results for p -Laplacian model problem

p -Laplacian model problem

$$\begin{aligned} -\alpha \Delta_p u &= 1 && \text{in } \Omega, \\ u &= 0 && \text{on } \partial\Omega. \end{aligned}$$

with $\alpha \Delta_p u := \operatorname{div}(\alpha |\nabla u|^{p-2} \nabla u)$.

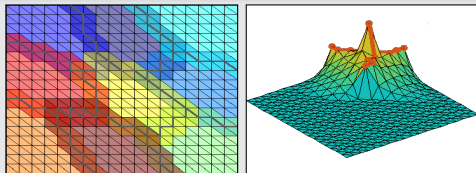
$p = 4$; $H/h = 16$; overlap $\delta = 1$

N	RASPEN solver	nonlin.		lin.
		outer it.	inner it. (avg.)	GMRES it. (sum)
9	NK-RAS	18	-	272
	RASPEN	5	25.2	89
25	NK-RAS	19	-	488
	RASPEN	6	28.3	172
49	NK-RAS	20	-	691
	RASPEN	6	27.3	232

⇒ Improved nonlinear convergence, but no scalability in the linear iterations.

Cf. Heinlein, Lanser (2020).

Two-level ASPEN & ASPIN methods



In two-level additive Schwarz preconditioned (in)exact Newton (ASPEN/ASPIN) in Heinlein, Lanser (2020), we consider

$$R_0^T T_0(u) + \sum_{i=1}^N P_i T_i(u) = 0$$

with

- corrections $T_i(u)$ as in the one-level case and
- the correction $T_0(u)$ given by a **nonlinear problem** in the **coarse space**

$$R_0 F(u - R_0^T T_0(u)) = 0;$$

via a **Galerkin projection**.

Results for p -Laplacian model problem

- 1-lvl One-level RASPEN
- 2-lvl A **Additive** two-level RASPEN
- 2-lvl M **Multiplicative** two-level RASPEN

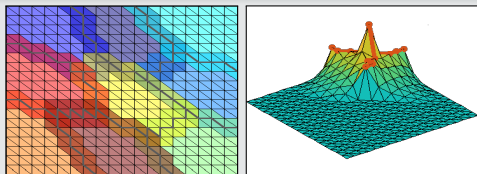
RGDSW coarse space: extensions computed using the tangent from the first linearization.

$p = 4; H/h = 16; \text{overlap } \delta = 1$					
N	RASPEN solver	nonlin.			lin.
		outer it.	inner it. (avg.)	coarse it.	GMRES it. (sum)
9	1-lvl	5	25.2	-	89
	2-lvl A	6	33.4	27	93
	2-lvl M	4	17.1	29	52
49	1-lvl	6	27.3	-	232
	2-lvl A	6	29.2	28	137
	2-lvl M	4	12.6	29	80

⇒ **Improved nonlinear convergence and scalability.**

Cf. Heinlein, Lanser (2020).

Three-level ASPEN & ASPIN methods



In three-level additive Schwarz preconditioned (in)exact Newton (ASPEN/ASPIN), we build the preconditioner recursively and consider

$$P_{00}^T T_{00}(u) + \sum_{j=1}^M P_{j0}^T T_{j0}(u) + \sum_{i=1}^N P_i T_i(u) = 0$$

with

level	correction	nonlinear problem
1	$T_0(u)$	$R_i F(u - P_i^T T_0(u)) = 0$
2	$T_{j0}(u)$	$R_{j0} F(u - P_{j0} T_{j0}(u)) = 0$
3	$T_{00}(u)$	$R_{j0} F(u - P_{00} T_{00}(u)) = 0$

Cf. Heinlein, Lanser, Klawonn (in prep.).

Results for p -Laplacian model problem

	additive		multiplicative	
	2-level	3-level	2-level	3-level
linear	M_A^{-1}	M_{AA}^{-1}	M_M^{-1}	M_{MM}^{-1}
nonlinear	\mathcal{F}_A	\mathcal{F}_{AA}	\mathcal{F}_M	\mathcal{F}_{MM}

$p = 4$; 16^2 subd.; 4^2 subr.; $H/h = 8$; overlap $\delta = 1$

RASPEM solver	nonlin.				lin.
	outer it.	subd. it. (avg./min/max)	subr. it.	coarse it.	GMRES it. (sum)
\mathcal{F}_A	6	23/16/46	-	36	90
\mathcal{F}_M	5	11/10/25	-	34	60
M_A^{-1}	24	-	-	-	381
M_M^{-1}	24	-	-	-	335
\mathcal{F}_{AA}	6	25/17/47	25/20/39	35	108
\mathcal{F}_{MM}	7	17/15/40	19/16/33	34	92
M_{AA}^{-1}	24	-	-	-	396
M_{MM}^{-1}	24	-	-	-	338

Multilevel domain decomposition-based architectures for physics-informed neural networks

Physics-Informed Neural Networks (PINNs)

In the **physics-informed neural network (PINN)** approach introduced by **Raissi et al. (2019)**, a neural network is employed to **discretize a partial differential equation**

$$\mathcal{N}[u] = f, \quad \text{in } \Omega.$$

PINNs use a **hybrid loss function**:

$$\mathcal{L}(\theta) = \omega_{\text{data}} \mathcal{L}_{\text{data}}(\theta) + \omega_{\text{PDE}} \mathcal{L}_{\text{PDE}}(\theta),$$

where ω_{data} and ω_{PDE} are **weights** and

$$\mathcal{L}_{\text{data}}(\theta) = \frac{1}{N_{\text{data}}} \sum_{i=1}^{N_{\text{data}}} (u(\hat{\mathbf{x}}_i, \theta) - u_i)^2,$$

$$\mathcal{L}_{\text{PDE}}(\theta) = \frac{1}{N_{\text{PDE}}} \sum_{i=1}^{N_{\text{PDE}}} (\mathcal{N}[u](\mathbf{x}_i, \theta) - f(\mathbf{x}_i))^2.$$

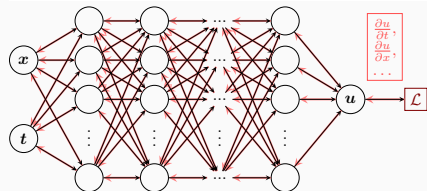
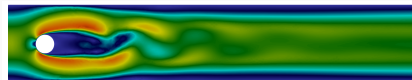
See also **Dissanayake and Phan-Thien (1994)**; **Lagaris et al. (1998)**.

Advantages

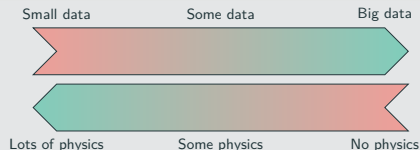
- **“Meshfree”**
- **Small data**
- **Generalization properties**
- **High-dimensional problems**
- **Inverse and parameterized problems**

Drawbacks

- **Training cost** and **robustness**
- **Convergence not well-understood**
- **Difficulties with scalability** and **multi-scale problems**



Hybrid loss



- **Known solution values** can be included in $\mathcal{L}_{\text{data}}$
- **Initial and boundary conditions** are also included in $\mathcal{L}_{\text{data}}$

Error Estimate & Spectral Bias

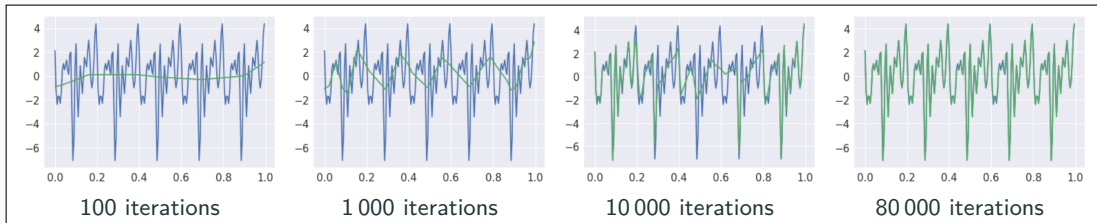
Estimate of the generalization error (Mishra and Molinaro (2022))

The generalization error (or total error) satisfies

$$\varepsilon_G \leq C_{\text{PDE}} \varepsilon_{\mathcal{T}} + C_{\text{PDE}} C_{\text{quad}}^{1/p} N^{-\alpha/p}$$

- $\varepsilon_G = \varepsilon_G(\mathbf{X}, \theta) := \|\mathbf{u} - \mathbf{u}^*\|_V$ **general. error** (V Sobolev space, \mathbf{X} training data set)
- $\varepsilon_{\mathcal{T}}$ **training error** (L^p loss of the residual of the PDE)
- N **number of the training points** and α **convergence rate of the quadrature**
- C_{PDE} and C_{quad} **constants** depending on the **PDE, quadrature, and neural network**

*Rule of thumb: “As long as the PINN is **trained well**, it also **generalizes well**”*



Rahaman et al., *On the spectral bias of neural networks*, ICML (2019)

Related works: Cao et al. (2021), Wang, et al. (2022), Hong et al. (arXiv 2022), Xu et al (2024), ...

A non-exhaustive literature overview:

- Machine Learning for adaptive BDDC, FETI–DP, and AGDSW: Heinlein, Klawonn, Lanser, Weber (2019, 2020, 2021, 2021, 2021, 2022); Klawonn, Lanser, Weber (2024)
- cPINNs, XPINNs: Jagtap, Kharazmi, Karniadakis (2020); Jagtap, Karniadakis (2020)
- Classical Schwarz iteration for PINNs or DeepRitz (D3M, DeepDDM, etc):: Li, Tang, Wu, and Liao (2019); Li, Xiang, Xu (2020); Mercier, Gratton, Boudier (arXiv 2021); Dolean, Heinlein, Mercier, Gratton (subm. 2024 / arXiv:2408.12198); Li, Wang, Cui, Xiang, Xu (2023); Sun, Xu, Yi (arXiv 2023, 2024); Kim, Yang (2023, 2024, 2024)
- FBPINNs, FBKANs: Moseley, Markham, and Nissen-Meyer (2023); Dolean, Heinlein, Mishra, Moseley (2024, 2024); Heinlein, Howard, Beecroft, Stinis (acc. 2024 / arXiv:2401.07888); Howard, Jacob, Murphy, Heinlein, Stinis (arXiv:2406.19662)
- DDMs for CNNs: Gu, Zhang, Liu, Cai (2022); Lee, Park, Lee (2022); Klawonn, Lanser, Weber (2024); Verburg, Heinlein, Cyr (subm. 2024)

An overview of the state-of-the-art in early 2021:



A. Heinlein, A. Klawonn, M. Lanser, J. Weber

Combining machine learning and domain decomposition methods for the solution of partial differential equations — A review

GAMM-Mitteilungen. 2021.

An overview of the state-of-the-art in mid 2024:



A. Klawonn, M. Lanser, J. Weber

Machine learning and domain decomposition methods – a survey

Computational Science and Engineering. 2024

Finite Basis Physics-Informed Neural Networks (FBPINNs)

In the **finite basis physics informed neural network (FBPINNs) method** introduced in **Moseley, Markham, and Nissen-Meyer (2023)**, we employ the **PINN** approach and **hard enforcement of the boundary conditions**; cf. **Lagaris et al. (1998)**.

FBPINNs use the **network architecture**

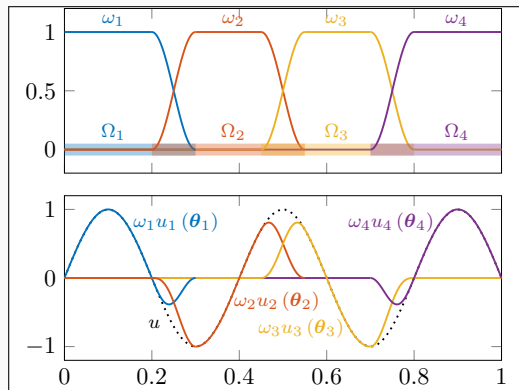
$$u(\theta_1, \dots, \theta_J) = \mathcal{C} \sum_{j=1}^J \omega_j u_j(\theta_j)$$

and the **loss function**

$$\mathcal{L}(\theta_1, \dots, \theta_J) = \frac{1}{N} \sum_{i=1}^N \left(n \left[\mathcal{C} \sum_{x_i \in \Omega_j} \omega_j u_j \right] (x_i, \theta_j) - f(x_i) \right)^2.$$

Here:

- **Overlapping DD:** $\Omega = \bigcup_{j=1}^J \Omega_j$
- **Partition of unity** ω_j with $\text{supp}(\omega_j) \subset \Omega_j$ and $\sum_{j=1}^J \omega_j \equiv 1$ on Ω



Hard enf. of boundary conditions

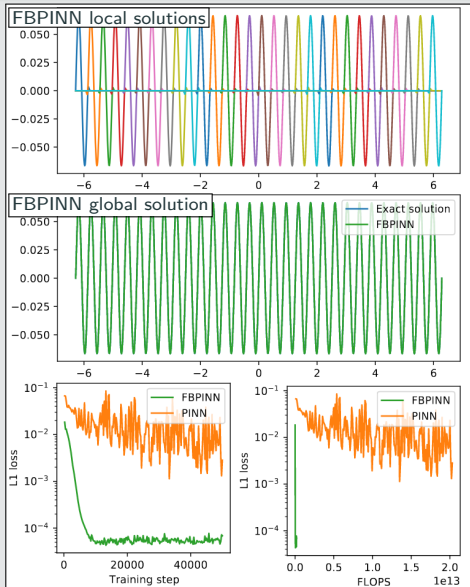
Loss function

$$\mathcal{L}(\theta) = \frac{1}{N} \sum_{i=1}^N \left(n \left[\mathcal{C} u \right] (x_i, \theta) - f(x_i) \right)^2,$$

with constraining operator \mathcal{C} , which **explicitly enforces the boundary conditions**.

Numerical Results for FBPINNs

PINN vs FBPINN (Moseley et al. (2023))

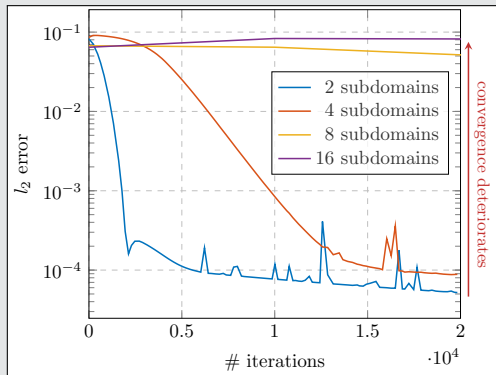
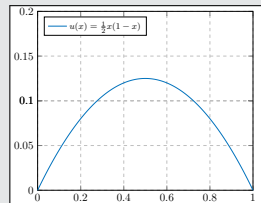


Scalability of FBPINNs

Consider the **simple** boundary value problem

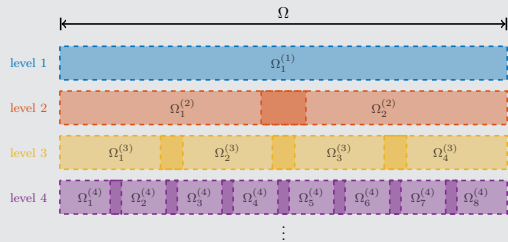
$$-u'' = 1 \text{ in } [0, 1],$$
$$u(0) = u(1) = 0,$$

which has the **solution**

$$u(x) = 1/2x(1 - x).$$


Multi-level FBPINNs (ML-FBPINNs)

ML-FBPINNs (Dolean, Heinlein, Mishra, Moseley (2024)) are based on a **hierarchy of domain decompositions**:



This yields the **network architecture**

$$u(\theta_1^{(1)}, \dots, \theta_{J^{(L)}}^{(L)}) = \sum_{l=1}^L \sum_{i=1}^{N^{(l)}} \omega_j^{(l)} u_j^{(l)}(\theta_j^{(l)})$$

and the **loss function**

$$\mathcal{L} = \frac{1}{N} \sum_{i=1}^N \left(n \left[\sum_{x_i \in \Omega_j^{(l)}} \omega_j^{(l)} u_j^{(l)} \right] (x_i, \theta_j^{(l)}) - f(x_i) \right)^2$$

Multi-Frequency Problem

Let us now consider the **two-dimensional multi-frequency Laplace boundary value problem**

$$-\Delta u = 2 \sum_{i=1}^n (\omega_i \pi)^2 \sin(\omega_i \pi x) \sin(\omega_i \pi y) \quad \text{in } \Omega,$$

$$u = 0 \quad \text{on } \partial\Omega,$$

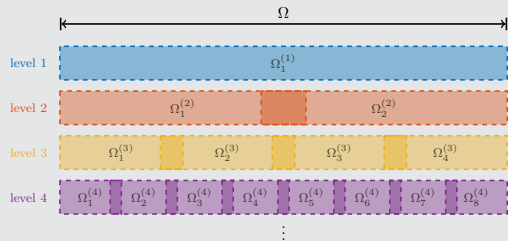
with $\omega_i = 2^i$.

For increasing values of n , we obtain the **analytical solutions**:



Multi-level FBPINNs (ML-FBPINNs)

ML-FBPINNs (Dolean, Heinlein, Mishra, Moseley (2024)) are based on a **hierarchy of domain decompositions**:



This yields the **network architecture**

$$u(\theta_1^{(1)}, \dots, \theta_{J^{(L)}}^{(L)}) = \sum_{l=1}^L \sum_{i=1}^{N^{(l)}} \omega_j^{(l)} u_j^{(l)}(\theta_j^{(l)})$$

and the **loss function**

$$\mathcal{L} = \frac{1}{N} \sum_{i=1}^N \left(n \left[\sum_{x_i \in \Omega_j^{(l)}} \omega_j^{(l)} u_j^{(l)} \right] (x_i, \theta_j^{(l)}) - f(x_i) \right)^2$$

Multi-Frequency Problem

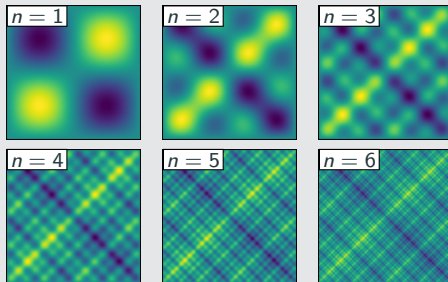
Let us now consider the **two-dimensional multi-frequency Laplace boundary value problem**

$$-\Delta u = 2 \sum_{i=1}^n (\omega_i \pi)^2 \sin(\omega_i \pi x) \sin(\omega_i \pi y) \quad \text{in } \Omega,$$

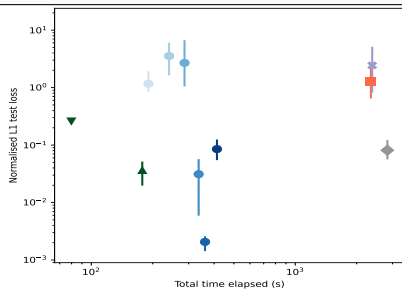
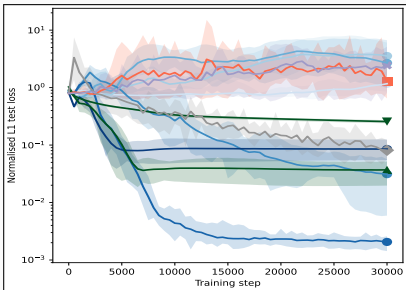
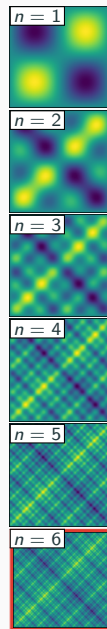
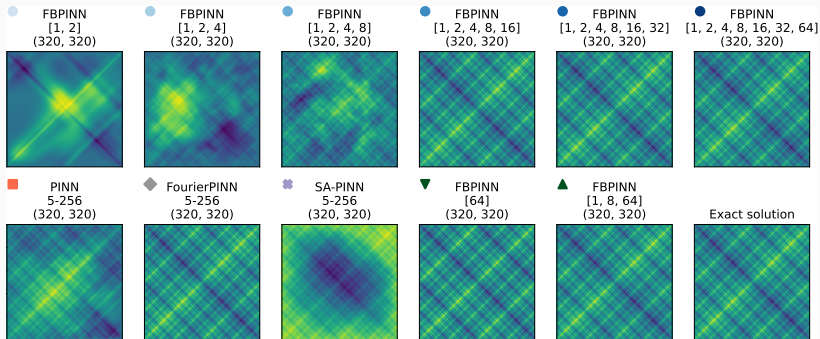
$$u = 0 \quad \text{on } \partial\Omega,$$

with $\omega_i = 2^i$.

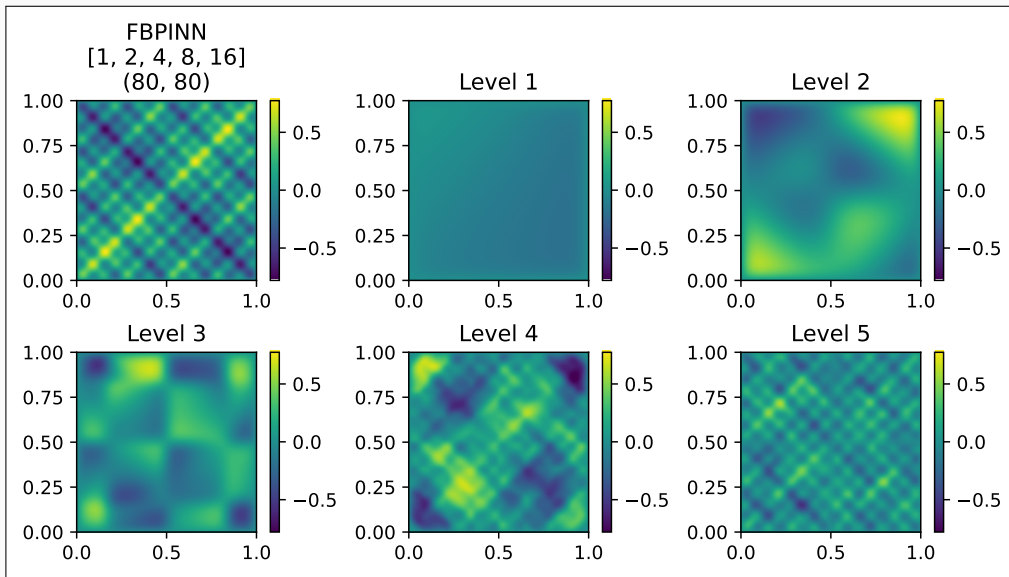
For increasing values of n , we obtain the **analytical solutions**:



Multi-Level FBPINNs for a Multi-Frequency Problem – Strong Scaling

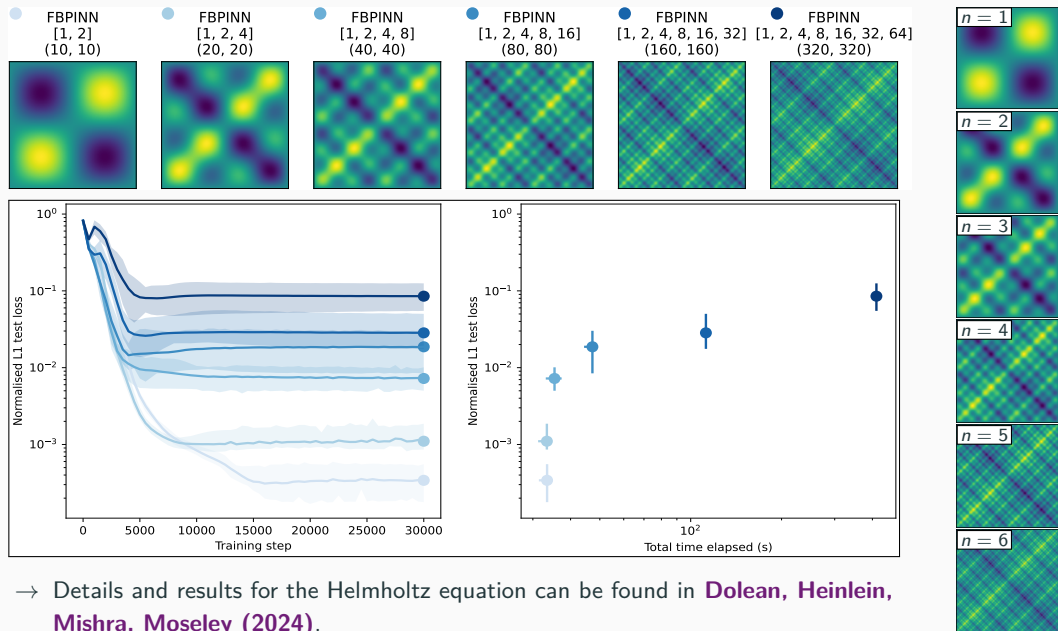


Multi-Frequency Problem – What the FBPINN Learns



Cf. [Dolean, Heinlein, Mishra, Moseley \(2024\)](#).

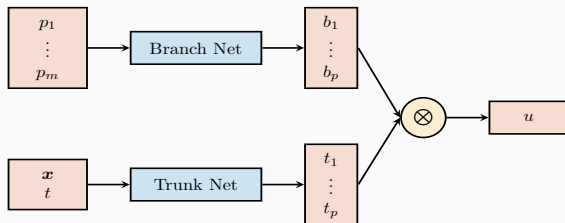
Multi-Level FBPINNs for a Multi-Frequency Problem – Weak Scaling



→ Details and results for the Helmholtz equation can be found in [Dolean, Heinlein, Mishra, Moseley \(2024\)](#).

Deep Operator Networks (DeepONets / DONs)

Neural operators learn operators between function spaces using neural networks. Here, we learn the **solution operator** of a initial-boundary value problem parametrized with p_1, \dots, p_m using **DeepONets** as introduced in **Lu et al. (2021)**.



Single-layer case

The DeepONet architecture is based on the **single-layer case** analyzed in **Chen and Chen (1995)**. In particular, the authors show **universal approximation properties for continuous operators**.

The architecture is based on the following ansatz for presenting the parametrized solution

$$u_{(p_1, \dots, p_m)}(\mathbf{x}, t) = \sum_{i=1}^p \underbrace{b_i(p_1, \dots, p_m)}_{\text{branch}} \cdot \underbrace{t_i(\mathbf{x}, t)}_{\text{trunk}}$$

Physics-informed DeepONets

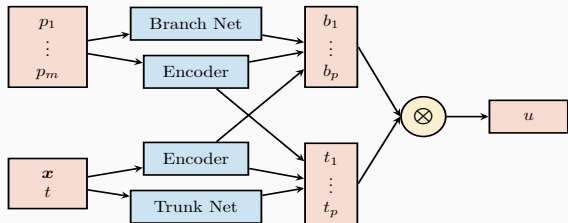
DeepONets are compatible with the PINN approach but **physics-informed DeepONets (PI-DeepONets)** are challenging to train.

Other operator learning approaches

- FNOs: **Li et al. (2021)**
- PCA-Net: **Bhattacharya et al. (2021)**
- Random features: **Nelsen and Stuart (2021)**
- CNOs: **Raonić et al. (arXiv 2023)**

Deep Operator Networks (DeepONets / DONs)

Neural operators learn operators between function spaces using neural networks. Here, we learn the **solution operator** of a initial-boundary value problem parametrized with p_1, \dots, p_m using **DeepONets** as introduced in **Lu et al. (2021)**.



Modified architecture

In our numerical experiments, we employ the **modified DeepONet architecture** introduced in **Wang, Wang, and Perdikaris (2022)**.

The architecture is based on the following ansatz for presenting the parametrized solution

$$u_{(p_1, \dots, p_m)}(\mathbf{x}, t) = \sum_{i=1}^p \underbrace{b_i(p_1, \dots, p_m)}_{\text{branch}} \cdot \underbrace{t_i(\mathbf{x}, t)}_{\text{trunk}}$$

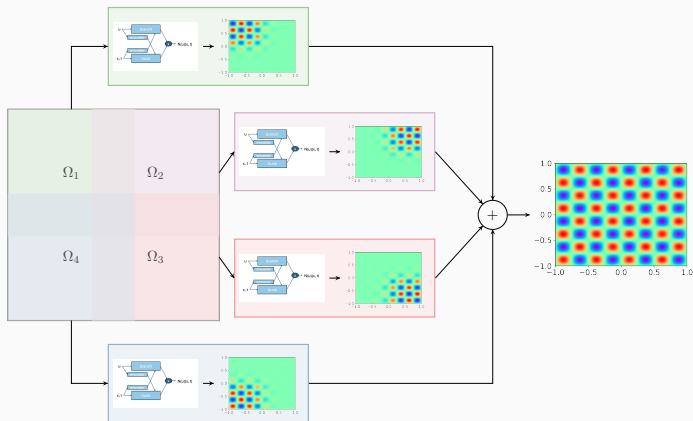
Physics-informed DeepONets

DeepONets are compatible with the PINN approach but **physics-informed DeepONets (PI-DeepONets)** are challenging to train.

Other operator learning approaches

- FNOs: **Li et al. (2021)**
- PCA-Net: **Bhattacharya et al. (2021)**
- Random features: **Nelsen and Stuart (2021)**
- CNOs: **Raonić et al. (arXiv 2023)**

Finite Basis DeepONets (FBDONs)



Howard, Heinlein, Stinis (in prep.)

Variants:

Shared-trunk FBDONs (ST-FBDONs)

The trunk net learns spatio-temporal basis functions. In ST-FBDONs, we use the **same trunk network for all subdomains**.

Stacking FBDONs

Combination of the **stacking multifidelity approach** with FBDONs.

Heinlein, Howard, Beecroft, Stinis (acc. 2024/arXiv:2401.07888)

Pendulum problem

$$\frac{ds_1}{dt} = s_2, \quad t \in [0, T],$$

$$\frac{ds_2}{dt} = -\frac{b}{m}s_2 - \frac{g}{L}\sin(s_1), \quad t \in [0, T],$$

where $m = L = 1$, $b = 0.05$, $g = 9.81$, and $T = 20$.

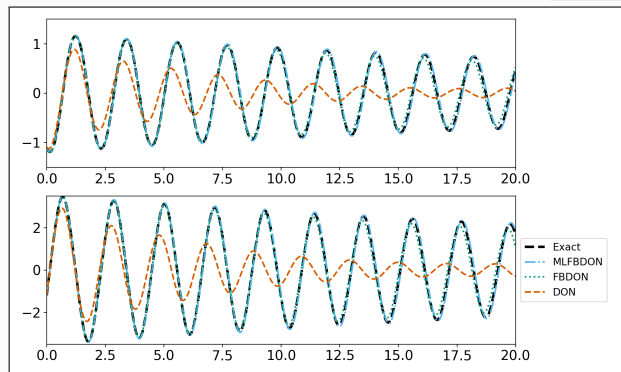
Parametrization

Initial conditions:

$$s_1(0) \in [-2, 2] \quad s_2(0) \in [-1.2, 1.2]$$

$s_1(0)$ and $s_2(0)$ are the also inputs of the branch network.

Training on 50 k different configurations



Mean rel. l_2 error on 100 config.

DeepONet	0.94
FBDON (32 subd.)	0.84
MLFBDON ([1, 4, 8, 16, 32] subd.)	0.27

Cf. [Howard, Heinlein, Stinis \(in prep.\)](#)

FBDONs – Wave Equation

Wave equation

$$\frac{d^2 s}{dt^2} = 2 \frac{d^2 s}{dx^2}, \quad (x, t) \in [0, 1]^2$$

$$s_t(x, 0) = 0, x \in [0, 1], \quad s(0, t) = s(1, t) = 0,$$

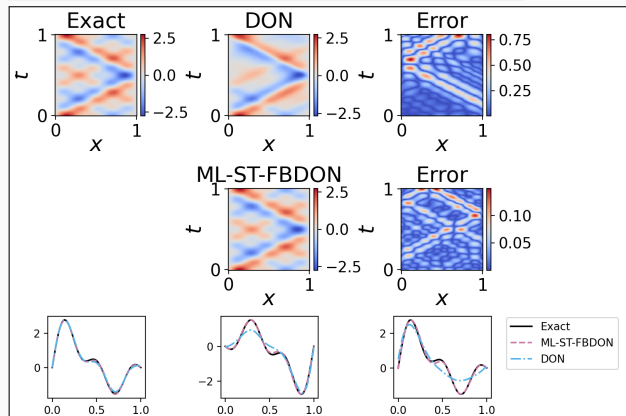
$$\text{Solution: } s(x, t) = \sum_{n=1}^5 b_n \sin(n\pi x) \cos(n\pi\sqrt{2}t)$$

Parametrization

Initial conditions for s parametrized by $b = (b_1, \dots, b_5)$ (normally distributed):

$$s(x, 0) = \sum_{n=1}^5 b_n \sin(n\pi x) \quad x \in [0, 1]$$

Training on 1000 random configurations.



Mean rel. l_2 error on 100 config.

DeepONet	0.30 ± 0.11
ML-ST-FBDON ([1, 4, 8, 16] subd.)	0.05 ± 0.03
ML-FBDON ([1, 4, 8, 16] subd.)	0.08 ± 0.04

→ Sharing the trunk network does not only save in the number of parameters but even yields **better performance**

Cf. **Howard, Heinlein, Stinis (in prep.)**

Co-organizers: Victorita Dolean (TU/e), Alexander Heinlein (TU Delft), Benjamin Sanderse (CWI), Jemima Tabbart (TU/e), Tristan van Leeuwen (CWI)

- **Autumn School** (October 27–31, 2025):
 - [Chris Budd](#) (University of Bath)
 - [Ben Moseley](#) (Imperial College London)
 - [Gabriele Steidl](#) (Technische Universität Berlin)
 - [Andrew Stuart](#) (California Institute of Technology)
 - [Andrea Walther](#) (Humboldt-Universität zu Berlin)
- **Workshop** (December 1–3, 2025):
 - 3 days with plenary talks (academia & industry) and an industry panel
 - Confirmed plenary speakers:
 - [Marta d'Elia](#) (Meta)
 - [Benjamin Peherstorfer](#) (New York University)
 - [Andreas Roskopf](#) (Fraunhofer Institute)



Centrum Wiskunde & Informatica



Join us for inspiring talks, hands-on sessions, and industry collaboration!

FROSch

- FROSch is based on the **Schwarz framework** and **energy-minimizing coarse spaces**, which provide **numerical scalability** using **only algebraic information** for a **variety of applications**

Multilevel neural network architectures

- **Domain decomposition-based architectures improve the scalability of PINNs to large domains / high frequencies, keeping the complexity of the local networks low.**
- As classical domain decomposition methods, **one-level FBPINNs are not scalable to large numbers of subdomains; multilevel FBPINNs enable scalability.**
- The multilevel FBPINN approach can also be **extended to operator learning.**

Thank you for your attention!



Topical Activity
Group

Scientific Machine
Learning

